J|A|C|S
COMMUNICATIONS

Published on Web 09/15/2004

Semiconductor-Encapsulated Peptide−Amphiphile Nanofibers

Eli D. Sone† and Samuel I. Stupp*

Department of Chemistry, Department of Materials Science & Engineering, and Feinberg School of Medicine, Northwestern University, 2220 Campus Drive, Evanston, Illinois 60208

Received January 5, 2004; E-mail: s-stupp@northwestern.edu

Controlling the structure and organization of inorganic materials on the nanoscale remains a goal of both scientific and technological importance for materials chemists. In this context, there is still much to learn from nature about how self-assembled organic templates can be used to nucleate and guide the growth of inorganic nanocrystals, as is the case for many biominerals.[1] It is possible to apply the concepts of biomineralization to synthetic minerals with interesting and potentially useful properties, such as semiconductors, as has been demonstrated by a number of groups including our own.[2] Here we describe an approach based on previously reported self-assembled nanofibers of a peptide−amphiphile (PA)[3] that we have found to be be effective substrates for nucleation and growth of cadmium sulfide (CdS) nanocrystals.

As detailed in previous work, PA **1** self-assembles at acidic pH into cylindrical fibers ∼6−8 nm in diameter, with the hydrophobic alkyl tails in the interior of the fibers.[3,4] These nanofibers can be cross-linked through disulfide bonds between interior cysteine groups to yield pH-stable fibers displaying on their surfaces the $S^{(P)}$RGD peptide sequence. Although the phosphoserine was originally incorporated into the sequence for its role as a promoter of nucleation of hydroxyapatite ($Ca_{10}(PO_4)_6(OH)_2$), we reasoned that Cd^{2+} might also be effectively sequestered by the fibers through coordination to the phosphate or acid groups. This would create a local supersaturation of Cd^{2+} ions, leading to preferred nucleation and growth of CdS nanocrystals within peptidic shells of the nanofibers upon introduction of a source of S^{2-}.

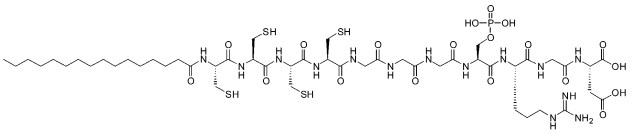

1

To test this hypothesis, we prepared dilute (10−50 μg/mL) aqueous suspensions of cross-linked fibers from 10 mg/mL gels, using a combination of mechanical agitation and sonication to break up the gel. Cadmium nitrate tetrahydrate ($Cd(NO_3)_2{\cdot}4H_2O$) in water was used as a source of Cd^{2+}, and the suspensions were subsequently exposed to hydrogen sulfide (H_2S) gas. Figure 1 shows transmission electron microscopy (TEM) micrographs of the resultant nanostructures formed when H_2S was diffused through suspensions containing various molar ratios of Cd^{2+}:PA. In systems containing modest amounts of cadmium (Figure 1a, Cd^{2+}:PA = 2.4:1), individual CdS nanocrystals ∼3−5 nm in diameter can be seen decorating the PA fibers. Many of the one-dimensional structures in the micrograph are ∼10 nm in width, consistent with single PA fibers made somewhat wider by outgrowth of CdS. In some cases, the fibers appear to be mineralized by two rows of CdS particles separated by a gap of ∼2−3 nm, which is the approximate dimension of the nanofiber's hydrophobic core. The observed pattern suggests that the PA fiber cross-section may be somewhat elliptical in shape, with the sharp ends perhaps mineralizing preferentially, although it may also be an artifact due to flattening of the fibers on the TEM grid. The lattice fringes imaged by high-resolution TEM of samples with the same Cd^{2+}:PA ratio (Figure 2) reveal that each particle is a single crystal. The spacings of these fringes correspond to various projections of the CdS zinc blende structure, which is consistent with our electron diffraction results (vide infra). We note that we did not observe any preferred orientation of the nanocrystals with respect to the fiber axis, in contrast with the results for hydroxyapatite (HA), in which we observed orientation of the crystallographic *c*-axis along the axis of the fiber.[3] As the HA orientation is presumably due to an epitaxial effect, the lack of orientation in CdS may be explained by the fact that the metal−metal distance in CdS (4.1 Å) is quite different from that in HA (6.9 Å), eliminating the possibility for epitaxial growth.

At an intermediate Cd^{2+}:PA ratio (Figure 1b, Cd^{2+}:PA = 24:1), PA fibers are completely encapsulated by CdS. The CdS layer appears to be made up of a continuous polycrystalline coating with 5−7 nm grains. Selected area electron diffraction (Figure 1b, left inset) confirmed that the mineral is CdS with the cubic zinc blende structure. Both coated single fibers and fiber-bundles are evident, with the width of the former (∼20 nm) indicating significant overgrowth of the fibers by the mineral. We note that there is a light stripe through the middle of the CdS/PA composite structures, as is highlighted in the right inset of Figure 1b. This feature results from a lower electron density core in the CdS tube, presumably due to the organic PA fiber. The 2−3 nm width of the stripe suggests that only the hydrophobic core of the PA fiber is unmineralized, while the more hydrophilic amino acids on its periphery are imbedded in the CdS.

While increasing the Cd^{2+}:PA ratio moderately leads to thicker CdS/PA composites, at sufficiently high ratios (Figure 1c, Cd^{2+}:PA = 240:1), the tubular CdS morphology is no longer observed. Rather, various-sized spherical aggregates of CdS nanocrystals appearing to have grown in solution can be seen, similar to what is observed in control mineralizations done without PA. Unmineralized PA fibers are also evident. Evidently, once PA coordination sites are saturated and enough Cd^{2+} ions exist in the solvent, the CdS is nucleated homogeneously.

We monitored the growth of CdS on the PA fibers by UV−vis absorbance spectroscopy at several time intervals after exposure of the suspensions to H_2S (see Supporting Information). For a sample with Cd^{2+}:PA ratio of 2.4:1, we initially observed (1 min after injection of H_2S) an absorption onset of 466 nm,[5] which is significantly blue-shifted from the value for bulk, zinc blende CdS of 515 nm.[6] After 20 min, the onset had gradually increased to 476 nm. According to Henglein and co-workers' experimentally determined relationship between absorption onset and CdS particle size,[7] this corresponds to particles initially ∼4 nm in diameter that

† Current address: Department of Structural Biology, Weizmann Institute of Science, Rehovot 76100, Israel.

10.1021/ja0499344 CCC: $27.50

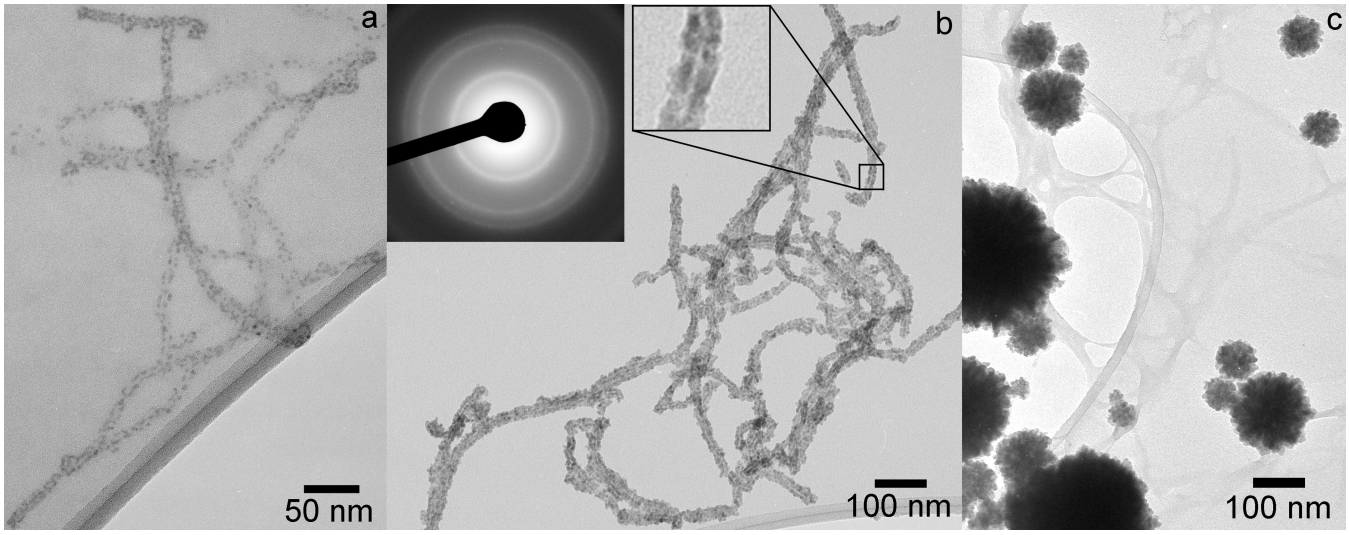

Figure 1. Bright field TEM micrographs of CdS mineralized suspensions of PA fibers at various Cd^{2+}:PA molar ratios: (a) Cd^{2+}:PA = 2.4:1; (b) Cd^{2+}:PA = 24:1. Left inset shows an electron diffraction pattern corresponding to the CdS zinc blende structure. Right inset shows an enlargement of a portion of an encapsulated fiber highlighting the strip of lower electron density through the middle corresponding to the hydrophobic core; (c) Cd^{2+}:PA = 240:1.

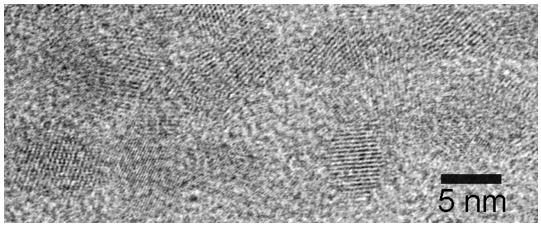

Figure 2. High-resolution TEM micrograph showing the lattice structure of CdS nanocrystals grown on a PA fiber. Fiber axis is parallel to the long axis of the micrograph.

grow to ~4.5 nm, consistent with the diameter range of 3−5 nm we measured by TEM 20 min after exposure to H_2S. The fact that the particles remain quantum-confined also supports our TEM data showing that some of the nanocrystals are spatially isolated in samples with this Cd^{2+}:PA ratio (Figure 2). In contrast, a control sample lacking PA fibers shows an initial absorption onset of 490, shifting to 500 nm in a similar time interval. The initial value corresponds to a particle size of ~6 nm, while the final value is nearly identical to the value for bulk wurtzite CdS of 499 nm,[8] indicating that the particles are no longer quantum-confined. Indeed, TEM of the control sample after 20 min (see Supporting Information) shows spheres of agglomerated particles ~5−10 nm in size with electron diffraction corresponding to the CdS wurtzite structure. The difference in polymorph between the templated CdS (zinc blende) and the nontemplated CdS of the control sample (wurtzite) provides clear evidence that the templated CdS is nucleated on the PA fibers themselves, rather than nucleating in solution and subsequently attaching to the fibers.

The robustness and pH-stability of cross-linked PA fibers make them potentially suitable for a variety of mineralization reactions, as illustrated by the metal sulfide semiconductor example described here. In addition, the chemistry on the periphery of the fibers can be readily tailored to give templates with specific affinities for different precursors, further expanding the spectrum of mineralization targets and thus potential applications.

Acknowledgment. This work was supported by the U.S. Department of Energy under Award No. DE-FG02-00ER45810. We are grateful for the use of the Electron Probe Instrumentation Center and the Keck Biophysics Facility at Northwestern University. E.D.S. is grateful to the Natural Sciences and Engineering Research Council of Canada for a post-graduate scholarship. We thank Krista L. Niece of our laboratory for synthesis of the PA and Dr. Elia Beniash for helpful discussions.

Supporting Information Available: UV−vis absorbance spectra of CdS on PA fibers; TEM micrograph and selected area diffraction pattern of CdS mineralized in a control sample. This material is available free of charge via the Internet at http://pubs.acs.org.

References

(1) Lowenstam, H. A.; Weiner, S. *On Biomineralization*; Oxford University Press: Oxford, 1989.
(2) (a) Braun, P. V.; Osenar, P.; Stupp, S. I. *Nature* **1996**, *380*, 325−328. (b) Coffer, J. L.; Bigham, S. R.; Li, X.; Pinizzotto, R. F.; Rho, Y. G.; Pirtle, R. M.; Pirtle, I. L. *Appl. Phys. Lett.* **1996**, *69*, 3851−3853. (c) Shenton, W.; Douglas, T.; Young, M.; Stubbs, G.; Mann, S. *Adv. Mater.* **1999**, *11*, 253−256. (d) Bekele, H.; Fendler, J. H.; Kelly, J. W. *J. Am. Chem. Soc.* **1999**, *121*, 7266−7267. (e) Sone, E. D.; Zubarev, E. R.; Stupp, S. I. *Angew. Chem., Int. Ed. Engl.* **2002**, *41*, 1705−1709. (f) Liang, H.; Angelini, T. E.; Ho, J.; Braun, P. V.; Wong, G. C. L. *J. Am. Chem. Soc.* **2003**, *125*, 11786−11787.
(3) Hartgerink, J. D.; Beniash, E.; Stupp, S. I. *Science* **2001**, *294*, 1684−1688.
(4) Hartgerink, J. D.; Beniash, E.; Stupp, S. I. *Proc. Natl. Acad. Sci. U.S.A.* **2002**, *99*, 5133−5138.
(5) Determined as the inflection point of the absorbance specrum.
(6) Adachi, S. *Optical Constants of Crystalline and Amorphous Semiconductors: Numerical Data and Graphical Information*; Kluwer Academic Publishers: Boston, 1999.
(7) (a) Spanhel, L.; Haase, M.; Weller, H.; Henglein, A. *J. Am. Chem. Soc.* **1987**, *109*, 5649−5655. (b) Henglein, A. *Chem. Rev.* **1989**, *89*, 1861−1873.
(8) Madelung, O., Ed. *Semiconductors: Basic Data*, 2nd revised ed.; Springer: Berlin, New York, 1996.

JA0499344